LATERAL VARIATIONS IN LUNAR WEATHERING PATINA ON CENTIMETER TO NANOMETER SCALES. S. K. Noble[1], L. P. Keller[2], R. Christoffersen[2] and Z. Rahman[2], [1]NASA GSFC Mail Code 691, Greenbelt MD 20771, sarah.k.noble@nasa.gov, [2]NASA JSC, Mail Code KR, Houston TX 77058.

Introduction: All materials exposed at the lunar surface undergo space weathering processes. On the Moon, boulders make up only a small percentage of the exposed surface, and areas where such rocks are exposed, like central peaks, are often among the least space weathered regions identified from remote sensing data [1]. Yet space weathered surfaces (patina) are relatively common on returned rock samples, some of which directly sample the surface of larger boulders. Because, as witness plates to lunar space weathering, rocks and boulders experience longer exposure times compared to lunar soil grains, they allow us to develop a deeper perspective on the relative importance of various weathering processes as a function of time.

Sample: Building upon our earlier work on patina-coated chips from lunar rock 76015 [2,3], we obtained a thin section (TS), 76015,10, which has a discontinuous patina coating extending over ~2 cm of the TS. The thin section provides a more extensive lateral and cross-sectional view to examine the nature of patinas on a much larger scale than our previous TEM work, which sampled patina coatings at the 10-30 µm scale.

Methods: The thin section was carbon coated and analyzed in BSE using the FEG-SEM at Johnson Space Center. Because a standard thin section is about 30 µm thick, FIB (Focused Ion Beam) sections, which are typically 5-20 µm thick, can be pulled directly from the thin section. This allows us to choose areas where the patina displays specific characteristics or unique features to further investigate in TEM, a considerable improvement over selecting based only on surface expression, as was the case with the rock chips. Three FIB sections were produced from the TS using the FEI Quanta 3D600 FIB at JSC.

TEM images and chemical maps were obtained using the JEOL 2500SE 200 keV field-emission scanning-transmission electron microscope (FE-STEM) at JSC. The FE-STEM is optimazed for compositional spectrum imaging using a large-area, thin window energy-dispersive X-ray (EDX) spectrometer. Spectrum images of the sample were acquired with a 4 nm probe whose dwell time was minimized to avoid beam damage and element loss/mobilization during mapping.

Discussion and Results: The patina, where present, is typically several micrometers thick, but ranges up to 10s of micrometers in places. The patina layer is far from continuous, fresh rock surfaces are exposed in many places, consistent with a complex equilibrium between the spatially non-uniform deposition by impact melts and vapors and destruction by micrometeorite cratering over time.

Two distinct types of patina are present, equivalent to the "classic" and "fragmental" classes of Wentworth et al [3]. Classic patina, typified by FIB#2 (Fig. 1), has been described in our previous studies of 76015 and other rock patinas [2,4]. It is composed of complex layers of small glass units and oftens contains micrometeorite craters and entrained mineral grains.

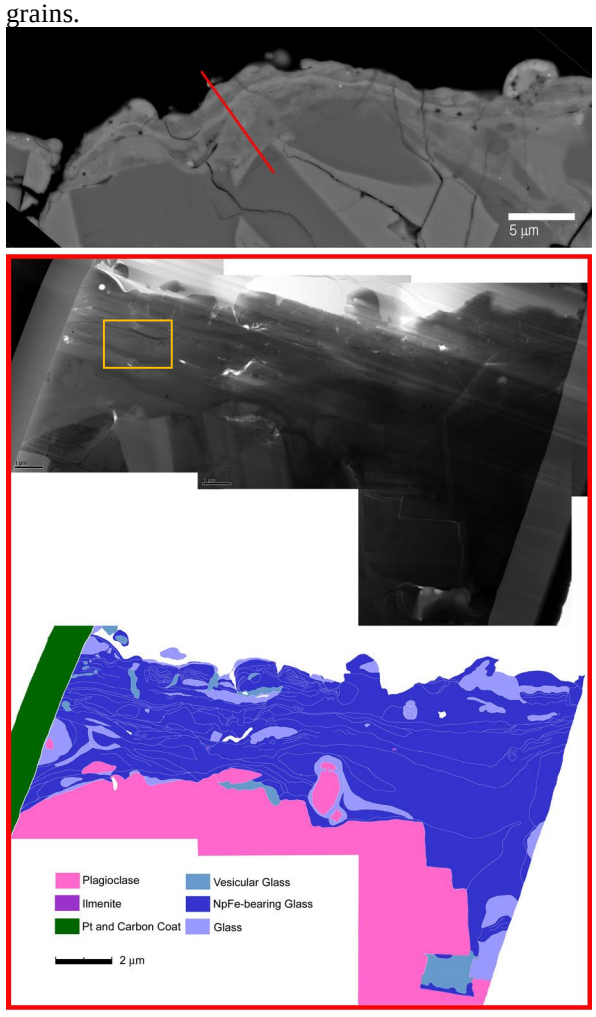

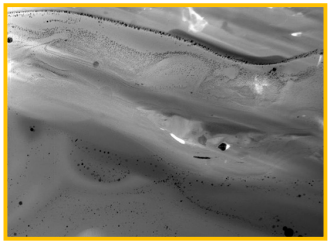

Figure 1. FIB#2 is an example of "classic" patina. The location of the FIB section is marked on the BSE image. The closeup at left shows the complex layers typical of these patinas.

The patina shown in Fig. 1 is ~ 5 µm thick and several distinct layers are apparent in the SEM image. The TEM analyses of the FIB section shows that the layers are themselves comprised of numerous (>40), small (µm-scale), npFe^0-bearing glass units with a wide range of compositions. The minerals beneath the patina coating contain high densities of solar-flare particle tracks and a lack of shock features. Interestingly, the track densities are comparable to the highest densities observed in lunar soil grains [5] and suggest that µm-thick patina layers accumulate rapidly, on a time scale similar to the exposure age lifetime of small regolith grains (on the order of 10^5 yrs).

Fragmental patina, seen in both FIB#1 and FIB#3 (Fig. 2) consists of fine-grained fragmental material welded to the surface of the rock. The individual grains constituting the fragmental patina are generally rounded to sub-angular and range in size from 10s of nanometers to about 2 micrometers. Most of the grains are glass that share a very similar chemistry (Fig. 3), suggesting they were deposited in a single event, presumably a local impact. There are also a few glass and mineral fragments with significantly different chemistry mixed in at the ~1-5% level. As in [3], we found that fragmental patina was largely concentrated in depressions. Additionally, it seemed to be confined to one small region of the TS, though it was the dominant patina type in that area, suggesting it may only occur in very localized areas. Fragmental patinas were frequently, though not always, capped with classic patina (e.g. FIB#1). The porosity of the fragmental breccias is highly variable, ranging from the densely-packed, low prorosity (~3%) endmember seen in FIB#1 to the high porosity (~33%) displayed by FIB#3, where grains barely touch their neighbors.

Conclusions: Two distinct types of space weathering patinas were identified from the 76015 TS. Both types of patina apparently develop rapidly on lunar rock surfaces. An optically thick layer of classic patina can be deposited on a ~10^5-year timescale, while the less common fragmental patina consists of deposits of material up to several micrometers from a single event. Rapid accumulation of optically-thick coatings is seemingly inconsistent with the detection of "fresh" surfaces of lunar rocks (e.g. central peaks) by VIS-NIR remote sensing techniques [e.g. 1].

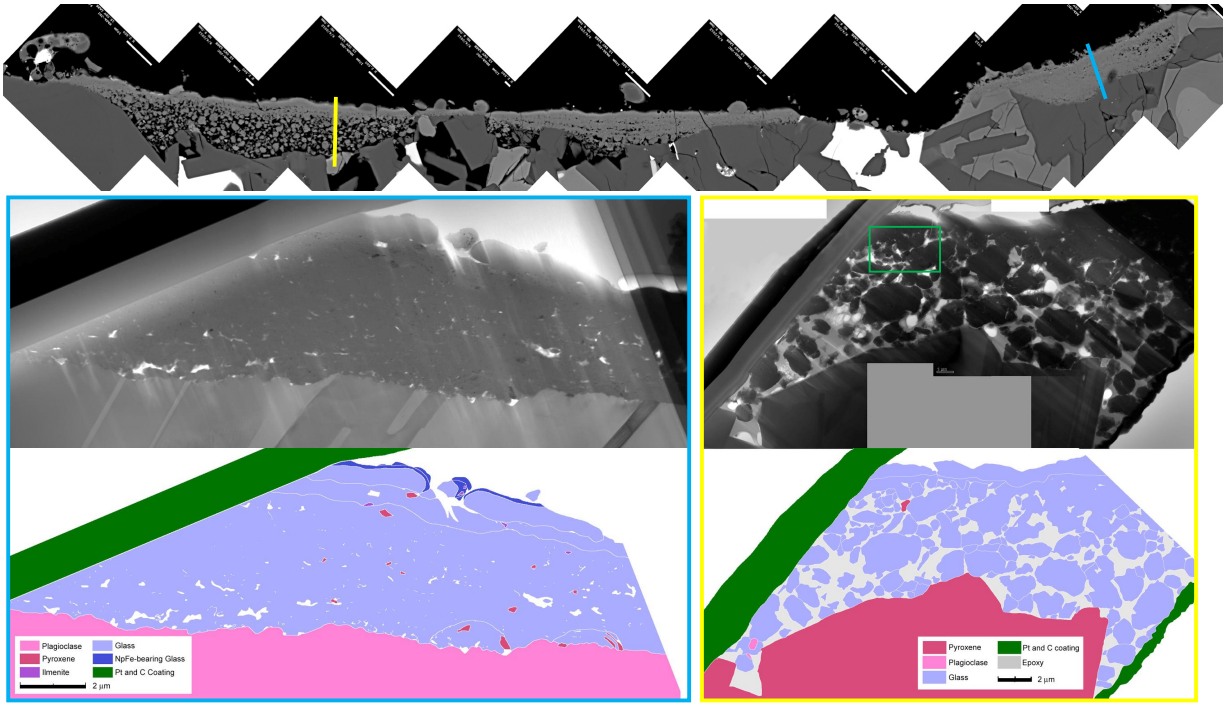

Figure 2. FIB#1 (left) and FIB#3 (right) are two examples of "fragmental" patina. The BSE image above shows where the sections were taken from.

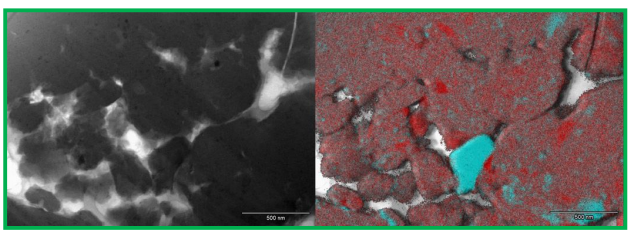

Figure 3. Chemical map from FIB#3, Mg=blue, Ca=red.

References: [1] Isaacson et al. (2011) *LPSCXLII*, #2556. [2] Noble S. et al. (2007) *LPSC XXXVIII*, #1359. [3] Wentworth S. et al. (1999) *MAPS* 34, 593-603. [4] Noble S. et al. (2012) *LPSCXLIII*, #1239. [5] Zhang, S. and Keller, L. P. (2011) *LPSCXLII*, #1947.